APPLIED MATERIALS AND TECHNOLOGY

Jamt.ejournal.unri.ac.id

Research Article

Synthesis of α-MnO_2@Mn_2O_3 and α-MnO_2 nanoparticles using tartaric/maleic acid and their enhanced performance in the catalytic oxidation of pulp and paper mill wastewater

Heni Sugesti[1,3,*], Barata Aditya Prawiranegara[2], Panca Setia Utama[1], Edy Saputra[1,*]

ABSTRACT: The Two MnOx, namely α-MnO_2@Mn_2O_3 and α-MnO_2 catalyst, were successfully synthesized using two different organic acids, tartaric and maleic acid, as a reduction in the redox process of KMnO4. The obtained catalysts are used in the AOP degradation reaction for paper mill effluent. The organic content in the effluent is analogous to the COD number in the effluent. The degradation process is depicted as a decrease in the COD number. The catalyst properties were characterized using X-ray diffraction (XRD), field emission scanning electron microscopy (FESEM), and N_2 adsorption-desorption. The obtained materials were then studied for peroxymonosulfate (PMS) activation as a sulfate radical source for COD removal reactions. The α-MnO_2@Mn_2O_3, which contains Mn (IV) and Mn (II, III), demonstrates an efficiency of nearly 75% COD removal when using a concentration of 0.3 gL^{-1}, surpassing the performance of the α-MnO_2 catalyst. The activation energy of the α-MnO_2@Mn_2O_3 is measured to be 11.4 kJ mol^{-1}.

Keywords: *Advanced oxidation processes, catalyst, degradation, pulp and paper mill effluent*

1. INTRODUCTION

With increased industrial production, contaminated effluent is released into nature [1]. Pulp and papermaking industries has become one of the largest industries and most water and energy consuming industries [2, 3]. The paper mill effluent, generate variety of the pollutants, both organic and small quantity of inorganic compound. The main compounds present in effluents are hemicelluloses, pectin, non-polar long-chain organic compound such as resin acids, lignans, and organic acids such as carboxylic acids in small quantities [4, 5]. Smaller molecular weight organic compound relatively easy to be removed using biodegradations methods, however high molecular weight organic compound such as lignin, cellulose, and hemicellulose are usually has more low biodegradable properties. Therefore, new treatment strategy must be emerged to tackle the problems [6]. One of the strongest candidates in water treatment process is advanced oxidation process or AOP [7, 8].

AOP were first proposed in the 1980s, which are described as oxidation process involving the generation of hydroxyl radicals ($OH^{\bullet}$) in quantity to effect water purification. In the next advancement, sulfate radicals ($SO_4^{\bullet-}$) was widely used [4, 9]. $SO_4^{\bullet-}$ is strong oxidant with standard oxidation potential of $E^o = 2.6$ eV. $SO_4^{\bullet-}$ could be activated from peroxymonoslufate (PMS; HSO_5^-) and peroxodisulfate (PDS; $S_2O_8^{2-}$) using certain catalyst in redox reaction [10, 11]. The catalyst itself usually transitional metals. The activation of $SO_4^{\bullet-}$ from HSO_5^- (PMS) and $S_2O_8^{2-}$ (PDS) reaction usually occurs [12]:

$$HSO_5^- + M^{n+} \rightarrow SO_4^{\bullet-} + H^+ + M^{n+1} \quad (1)$$

$$S_2O_8^{2-} + M^{n+} \rightarrow SO_4^{\bullet-} + SO_4^{2-} + M^{n+1} \quad (2)$$

The most frequently used metals include Ferric Fe(II) and Fe(III) ions, and manganese Mn(II), Mn(III), Mn(IV), and Mn(II, III), and Cobalt Co(II), Co(III), and Co(II, III) [13, 14]. Manganese based AOP catalysts have been studied exten-

OPEN ACCESS

Affiliation

[1]Department of Chemical Engineering, Riau University, Pekanbaru 28293, Indonesia.
[2]Department of Chemistry, Faculty of Mathematics and Natural Sciences Universitas Riau, Pekanbaru 28293, Indonesia.
[3]Chemical Engineering Department, Politeknik Negeri Sriwijaya, Palembang, 30139, Indonesia.

***Correspondence**
Email: henisugesti@polsri.ac.id (H.S); edy.saputra@eng.unri.ac.id (E.S)

ORCID
Heni Sugesti: 0009-0003-6069-5334
Barata Aditya Prawiranegara: 0000-0003-0023-8492
Panca Setia Utama: 0000-0002-6829-1321
Edy Saputra: 0000-0001-6430-9072

Received: January 09, 2025
Revised: February 24, 2025
Accepted: March 05, 2025

How to cite: Sugesti, H., Prawiranegara, B., A., Utama, P., S., & Saputra, E.. (2025). Synthesis of α-MnO_2@Mn_2O_3 and α-MnO_2 nanoparticles using tartaric/maleic acid and their enhanced performance in the catalytic oxidation of pulp and paper mill wastewater. *Journal of Applied Materials and Technology*, 6(1), 30–36. https://doi.org/10.31258/Jamt.6.1.30-36.

sively in recent decade due their physical and chemical properties. For instances, manganese oxide, has better performance in wider range of pH compared to Iron oxides to activate radicals [15-17]. Recent studies also stated physiochemical properties of manganese oxides such as crystal structures, oxidation states, event morphologies of the MnOx can significantly affect their effectiveness and performance in AOP reaction [18-21]. The reactivity of the manganese-based catalysts exhibited in an order of Mn_3O_4 > Mn_2O_3 > MnO_2 which was correlated with oxygen mobility in the catalyst [20]. To synthesized different physiochemical properties of the MnOx, many factors were involved. Temperature, reducing agent, reaction time, and solvent polarity were affected the oxidation state and crystal structure of the MnOx [22].

In water treatment AOP reaction, MnOx was usually activated PMS, PDS, even H_2O_2 to produce radicals required to oxidize the organic pollutant contained in the waste-water [23, 24]. Saputra, 2013, using different phase of MnO_2; α-, β-, and γ-MnO_2 with Oxone® to degrade phenol in aqueous solutions. The synthesized α-MnO_2 has activation energy around 21.9 $kJmol^{-1}$ for phenol degradation [19]. PDS activation using MnOx was done by few studies for removal different organic pollution such as phenol and nitrobenzene. It's believed that in PDS system beside $SO_4^{\bullet-}$, $OH^{\bullet}$ was also play strong role in degradation of organic pollutant [25, 26].

In this study, different MnO_2 catalysts were synthesized using maleic acid and tartaric acid which are α-MnO_2 and α-MnO_2@Mn_2O_3. The catalysts were synthesized using hydrothermal methods. The physiochemical properties of the catalysts were characterized using XRD, FESEM, and BET. The performance both of the catalysts were tested to degrade paper mill effluent pollutant using PMS as oxidant.

2. EXPERIMENTAL SECTIONS

2.1. Synthesis of α-MnO_2. The α-MnO_2 was prepared by reducing Potassium Permanganate ($KMnO_4$, Merck) with Maleic Acid ($C_4H_4O_4$, Sigma-Aldrich). $KMnO_4$ and $C_4H_4O_4$ were dissolved separately using deionized water with a molar ratio of 1:3 then mixed and stirred to produce precipitate in the form of blackish-brown particles. The precipitate is filtered accompanied by rinsing with non-ionized water, followed by storage and conditioning for 24 hours at room temperature. After storage at room temperature for 24 hours, it is then calcined at a temperature of 400°C for 4 hours with a heating rate of 3°C min^{-1} to form of α-MnO_2.

2.2. Synthesis of α-MnO_2@Mn_2O_3. The α-MnO_2@Mn_2O_3 was prepared by reducing Potassium Permanganate ($KMnO_4$, Merck) with tartaric Acid ($C_4H_6O_6$, Sigma-Aldrich). $KMnO_4$ and $C_4H_4O_4$ were dissolved separately using deionized water with a molar ratio of 1:3 then mixed and stirred to produce precipitate in the form of blackish-brown particles. The precipitate is filtered accompanied by rinsing with non-ionized water, followed by storage and conditioning for 24 hours at room temperature. After storage at room temperature for 24 hours, it is then calcined at a temperature of 300°C for 4 hours with a heating rate of 3°C min^{-1} to form a precursor. The precursor was then calcined again at a temperature of 400°C for 4 hours and formed a catalyst α-MnO_2@Mn_2O_3.

2.3. Catalyst performance in paper mill effluent degradation. α-MnO_2 and α-MnO_2@Mn_2O_3 was compared to determine the best catalyst in AOP reaction. Pulp and paper mill effluent degradation was done in a 1 L glass reactor with a magnetic stirrer, heater, and temperature controller. The reaction condition for COD removal were: Effluent volume of 1 L, stirrer speed of 400 RPM, catalyst dosage of 0.4 gL^{-1}, PMS concentration of 2 gL^{-1}, and temperature of 25°C, and reaction time of 180 min. for every predetermined time, 5 mL sample was taken out for COD analysis using COD reactor Hach DRB200, USA. To understand the effect of the catalyst, PMS was used without the presence of the catalyst. Adsorption test was done using the catalysts alone without the oxidant. The most effective catalyst from the test was utilized for further studies to examine the impact of catalyst dosage, PMS dosage, and temperature on the degradation of paper mill effluent. The effect of catalyst dosage (0.1, 0.2 and 0.3 gL^{-1}); PMS dosage(0.4, 0.8, 1.6 gL^{-1}); and temperature (30, 40, and 50°C).

2.4. Analysis and characterization of the catalyst. Paper mill effluent's COD was tested before and after degradation process according to SNI 6986.73:2009 parameter. XRD characterization was performed using a Rigaku Miniex Goniometer at 30 kV and 15 mA, using Cu Kα radiation at a step size of 0.01°. N_2 adsorption-desorption was applied to measure the surface area and pore size of the catalyst, according to the Brunauer-Emmet-Teller (BET) and Barrett, Joyner, and Halenda (BJH) methods using Quantachrome Nova 4200e, USA, Boynton Beach, Florida, USA. Catalyst morphology was characterized using the field emission scanning electron microscope JEOL Type JSM-6510LA, Japan.

3. RESULT AND DISCUSSION

3.1. The paper mills effluent analysis. Paper mill waste is collected from the wastewater treatment process. The obtained effluent was analyzed and found to have an initial COD content of 1,119.6 mgL^{-1}. According to the Indonesian National Standard Regulation (SNI), the maximum allowable COD limit for discharge into water bodies is 350 mgL^{-1} [27]. Consequently, the COD levels in the collected waste substantially exceed the permissible standard.

3.2. Characterization of the catalysts. Two catalyst was synthesized using two different small organic acids which are maleic and tartaric acid demonstrated two different crystal structures. The XRD patterns of the obtained catalysts exhibit two distinct profiles, as shown in Figure 1. The manganese oxides catalyst synthesized using maleic acid shows XRD peak patterns of 12.6°, 18.05°, 28.6°, °, 41.9°, 59.9°, 65.22° and 69.51°. The pattern is in accordance to tetragonal α-MnO_2 (JCPDS No. 044-0141) [28]. Manganese oxide synthesized using tartaric acid has mixed of dual phase of α-MnO_2 12.6°, 28.6°, 41.9°, and 59.9° with the additional of α-Mn_2O_3 at the peaks 23.13°, 32.95°, and 35.68° of cubic phase of α-Mn_2O_3 (JCPDS No. 41-1442) [29].

The two phase of the catalyst α-MnO_2@α-Mn_2O_3 consists of Mn (II, III) as the Mn_2O_3 and Mn(IV) of α-MnO_2 was the product of reacting MnO_4^- ion with tartaric acid as an organic reductor. The reaction mechanism for the formation of α-MnO_2@Mn_2O_3 is depicted in Scheme 1 [16]. Tartaric acid will proceed into an ester complex with MnO_4^- ion. Ester complex will undergo oxi-

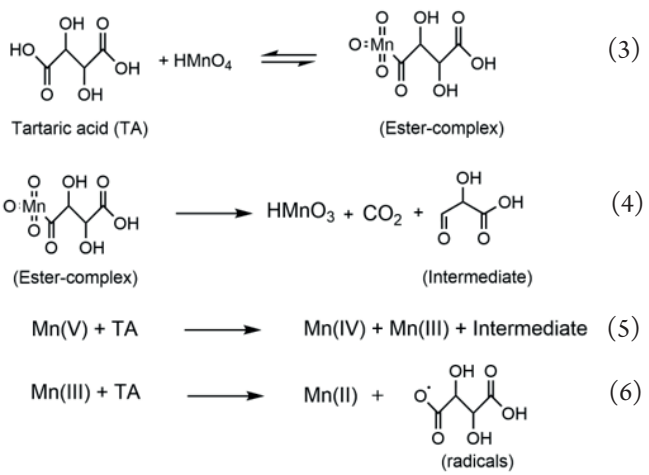

Scheme 1. Reaction mechanism of α-MnO_2@Mn_2O_3 formation.

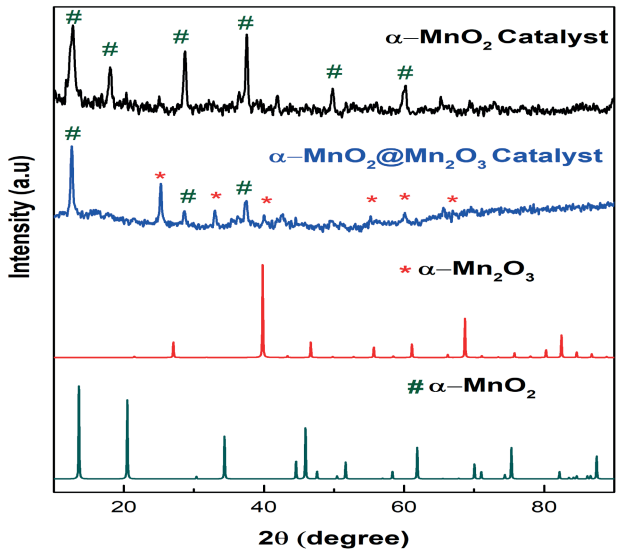

Figure 1. XRD patterns of α-MnO_2@α-Mn_2O_3 and α-MnO_2.

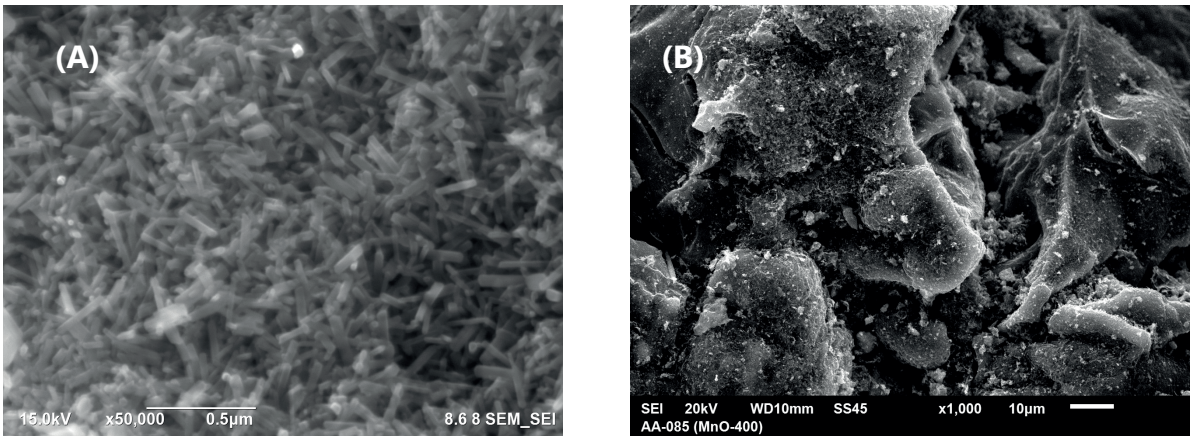

Figure 2. SEM images of α-MnO_2@α-Mn_2O_3 (A) nd α-MnO_2 (B).

dative decomposition into the formation of Mn(V), CO_2 and an intermediate (step 3). The next step, Mn(V) reacts with the TA, to produce Mn(IV) and Mn(III) and intermediate. Further redox reaction transform Mn(III) onto Mn(II). In contrast, maleic acid does not exhibit the same reduction strength as tartaric acid to convert $KMnO_4$ into the Mn(III) and Mn(II) phases.

The morphology of the catalyst was studied using SEM. SEM images of the catalyst were recorded in (Figure 2 A and B). α-MnO_2@α-Mn_2O_3 (Figure 2 A) existed in form of nanorods with length around 100-150 nm [30]. Meanwhile, α-MnO_2 (Figure 2 B) has less defined regular phase morphology.

Figure 3 shows N_2 adsorption isotherms and pore size distributions of the two manganese oxides catalysts (α-MnO_2@α-Mn_2O_3 and α-MnO_2). The surface area and pore volumes are given in Table 1. As we can see, α-MnO_2 has larger surface area which is 46.8 m^2g^{-1} and pore volume of 0.158 cm^3g^{-1}. α-MnO_2@α-Mn_2O_3 has smaller surface area 3.86 m^2g^{-1} with the pore volume of 0.078 cm^3g^{-1}. both of them have with type IV BET isotherm with hysteresis loop, meaning the catalysts have mesoporous pore system. the smaller surface area of α-MnO_2@α-Mn_2O_3 is because of the crystal multiphase structure. the nature of multiphase crystal tends to have aggregation of the crystal bulk and make the bigger crystal size, compared to the monophase crystal structure of MnO_2 which tends to be smaller in crystal size [31].

Table 1. Surface area and pore volume of α-MnO_2@α-Mn_2O_3 and α-MnO_2.

Catalyst	BET surface area (m^2g^{-1})	Pore volume (cm^3g^{-1})
α-MnO_2	46.8	0.158
α-MnO_2@α-Mn_2O_3	3.86	0.078

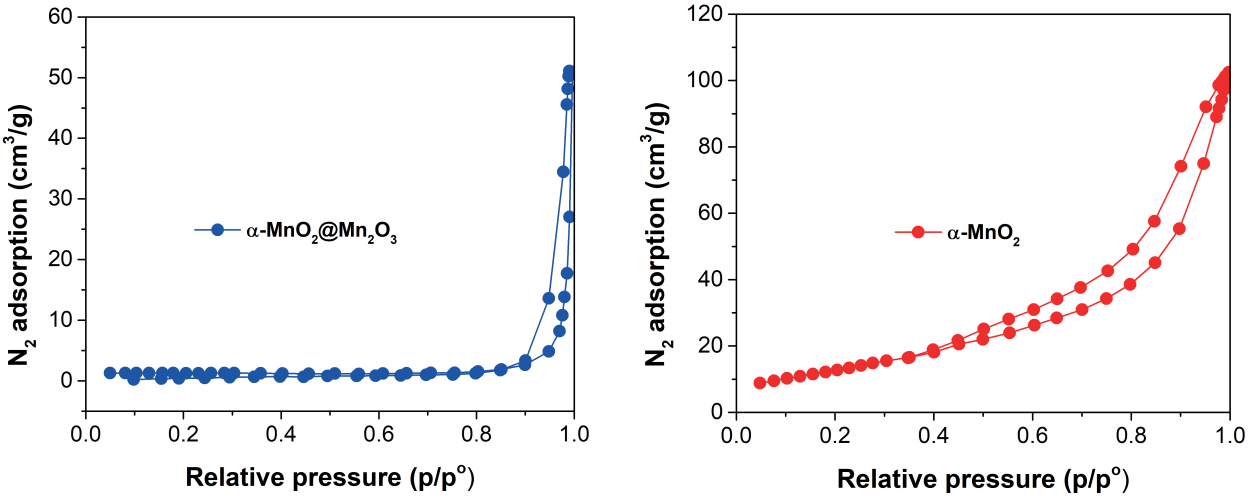

Figure 3. N_2 adsorption-desorption isotherm α-MnO_2@Mn_2O_3 and α-MnO_2.

3.3. Preliminary studies of COD removal. Figure 4 shows the performance of the catalysts for COD removal, as expected, COD degradation using only PMS showed no significant COD removal. Sulfate radical needs to be activated using catalyst before it could react with organic species. The adsorption process of the organic effluent is also negligible by using α-MnO_2 and α-MnO_2@Mn_2O_3. As those catalysts have substantially low surface area. The COD degradation kinetics are investigated using pseudo-first-order models as illustrated in Equation 7 [32].

$$C_{COD_t} = C_{COD_o} \cdot e^{-k_{obs} \cdot t} \quad (7)$$

where C_{COD} and C_{COD_o} are the COD concentration at a different time (t) and initial time (t_o), k_{obs} is the observed reaction rate constant. The α-MnO_2 catalyst has around 44.1% of COD removal efficiency with observed reaction rate constant of 0.042 min^{-1}. On the other hand, α-MnO_2@Mn_2O_3 exhibits better degradation efficiency, achieving 71.9% COD removal with an observed reaction rate of 0.067 min^{-1}. This indicates that the reaction is not related to surface area (Table 1). Previous study conducted by Saputra, various oxidation states of MnOx has different efficiency in sulfat radicals' activation from PMS. In this study, PMS activation rates as it follows Mn_2O_3>MnO>Mn_3O_4>MnO_2 [20]. α-MnO_2@Mn_2O_3 has better activity compared to the α-MnO_2 alone is because multi-valent Mn component Mn(III) and Mn(IV) are present in α-MnO_2@Mn_2O_3. The proposed mechanism of PMS activations is [33]:

$$HSO_5^- + Mn_2O_3 \rightarrow 2MnO_2 + SO_4^{\bullet-} + H^+ \quad (8)$$

$$HSO_5^- + 3Mn_2O_3 \rightarrow 2Mn_3O_4 + SO_5^{\bullet-} + OH^- \quad (9)$$

$$HSO_5^- + 2MnO_2 \rightarrow Mn_2O_3 + SO_5^{\bullet-} + OH^- \quad (10)$$

$$SO_4^{\bullet-} + H_2O \rightarrow OH^{\bullet} + H^+ + SO_5^{2-} \quad (11)$$

$$\text{Organic Pollutant}_{(COD)} + \text{Radicals}\ (SO_4^{\bullet-} + SO_5^{\bullet-} + OH^{\bullet}) \rightarrow \text{Intermediate} \rightarrow CO_2 + H_2O \quad (12)$$

As from the mechanism above, α-MnO_2@Mn_2O_3 with the presence of Mn_2O_3 will produce directly both $SO_4^{\bullet-}$ and $SO_5^{\bullet-}$, instead of α-MnO_2 that only have MnO_2 in the catalyst structure that only produce $SO_5^{\bullet-}$ that has less activity compared to $SO_4^{\bullet-}$ in COD removal process. As the best catalyst is α-MnO_2@Mn_2O_3, the catalyst then uses in the next process for further investigation.

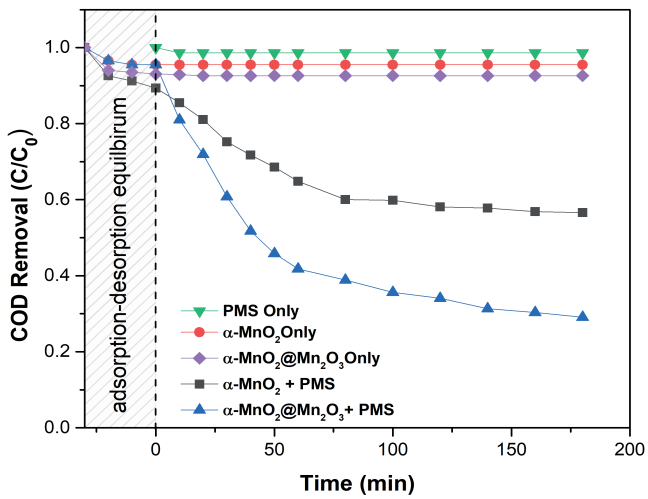

Figure 4. Comparison of COD removal of paper mill effluent profiles versus time on various prepared MnOx catalyst. Condition of Reaction: C_{COD_O} = 1,119 mgL^{-1}; [PMS] = 1.6 gL^{-1}; catalyst dosage: 0.3 gL^{-1}; Temp: 30°C.

3.4. Effect of reaction parameters on COD removal on α-MnO_2@Mn_2O_3 catalyst. Investigation regarding various effect on COD removal of paper mill effluent were carried out. Effect on catalyst loading in COD removal were investigated in Figure 5. COD removal efficiency was increased as the catalyst dosage increased. The best COD removal efficiency achieved by using the 0.3 gL^{-1} catalyst dosage, COD removal could be achieved at 71.82% with observed reaction rate of 0.067 min^{-1}. Lesser catalyst dosage at 0.2 gL^{-1} and 0.1 gL^{-1} achieved COD removal efficiency of 49.2% and 17.6% with observed reaction rate of 0.0036 min^{-1} and 0.0014 min^{-1} in respective order. The increased amount of the catalyst will promote the radical production, since the more active sites available in the catalytic process. As the more radical available, the more increased the rate of COD removal [34, 35].

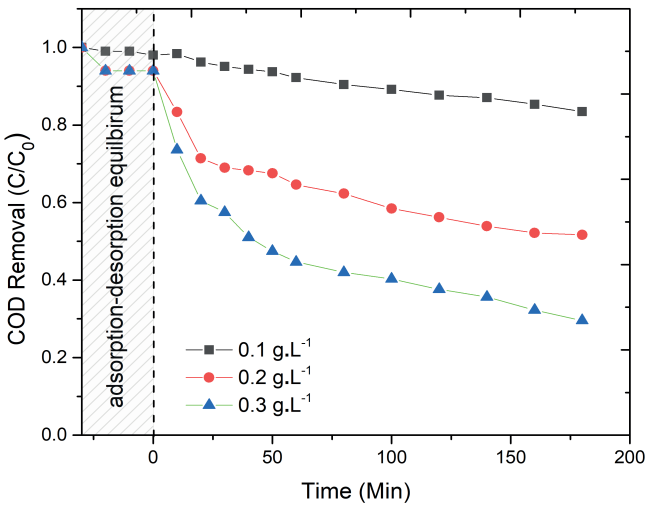

Figure 5. Comparison of COD removal of paper mill effluent profiles versus time on various catalyst loading. Condition of Reaction: C_{CODO} = 1,119 mgL^{-1}; [PMS] = 1.6 gL^{-1}; Temp: 30°C.

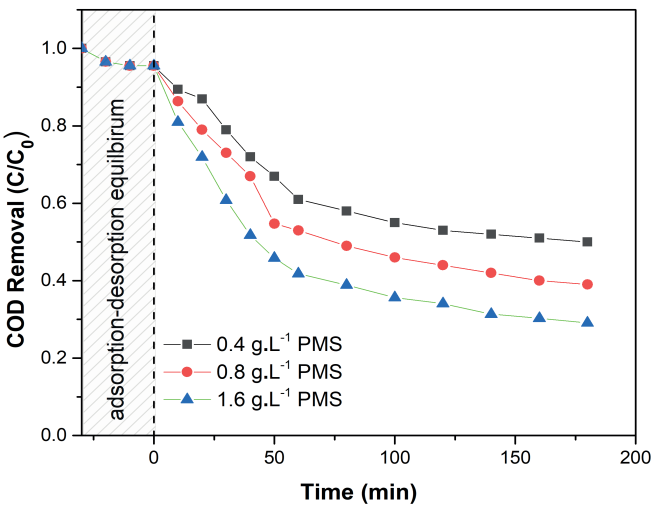

Figure 6. Comparison of COD removal of paper mill effluent profiles versus time on various PMS concentrations. Condition of Reaction: C_{CODO} = 1,119 mgL^{-1}; catalyst dosage: 0.3 gL^{-1}; Temp: 30°C.

Figure 6 shows the COD removal process at different oxidant concentrations. As it showed that increasing the concentration of PMS in solution, the COD removal efficiency also increased. The highest efficiency of COD removal was obtained at 1.6 gL^{-1} of PMS with 71.9% of COD removal (k_{obs}= 0.067 min^{-1}) compared to 51.3% (k_{obs} = 0.052 min^{-1}) and 44.1% of COD removal efficiency with observed reaction rate constant of (k_{obs}) 0.042 min^{-1} for 0.8 gL^{-1} and 0.4 gL^{-1} of PMS respectively. The more PMS available, directly involved in the radical production. Since, the available PMS will be activated on the surface of the catalyst to produce sulfate radicals. Therefore, in this study the more available PMS, the more radical will be produce to reduce the COD value in the solution [35].

The radical degradation of the organic materials is affected by the temperature, many of them considered as endothermic reactions. Figure 7 shows that the increase of the COD removal efficiency as the temperature increased. At the 50°C the COD removal efficiency was obtained at 59.1% at 60 minutes. However, at 40°C and 30°C the removal efficiency was reduced at 57.3% and 51.2% as respected order. Therefore, the COD removal of paper mill effluent is endothermic reaction. The reaction kinetics for each reaction were measured as illustrated in Equation 7 [36]. Where k_{obs} is the observed first order rate constant of COD removal. Data fitting using exponential equation shows that the paper mills effluent COD removal is apparent to be first order reactions. The rate kinetic constants for each temperature, obtained from Equation 7, are presented in Table 2.

Table 2. Catalyst activation energy and rate kinetic constant.

Catalyst	Temperature (°C)	k_{obs} (min^{-1})	Ea (kJ mol^{-1})
	30	0.067	
α-MnO_2@Mn_2O_3	40	0.07	11.4
	50	0.087	

The activation energy of the catalyst was determined by utilizing an Arrhenius plot of the kinetic constant, as depicted in the inset of Figure 7. This process involved a linear correlation with the Arrhenius equation, as illustrated in Equation 8 [37].

$$\ln k = \ln A - \frac{E_a}{RT} \quad (8)$$

The activation energy (Ea) of the catalyst could be approached. As it calculated, the activation energy of the α-MnO_2@Mn_2O_3 is 11.4 kJ mol^{-1} (Table 2). α-MnO_2@Mn_2O_3 has lower activation energy in COD removal reaction compared to MnO_2 only based catalyst with 39.9 kJ mol^{-1} [38], Co based with 20.6 kJ mol^{-1} [39], and carbon composite such as MOFs-derived C@Cu-Ni catalyst with the activation energy of 36.6 kJ mol^{-1} [40] .

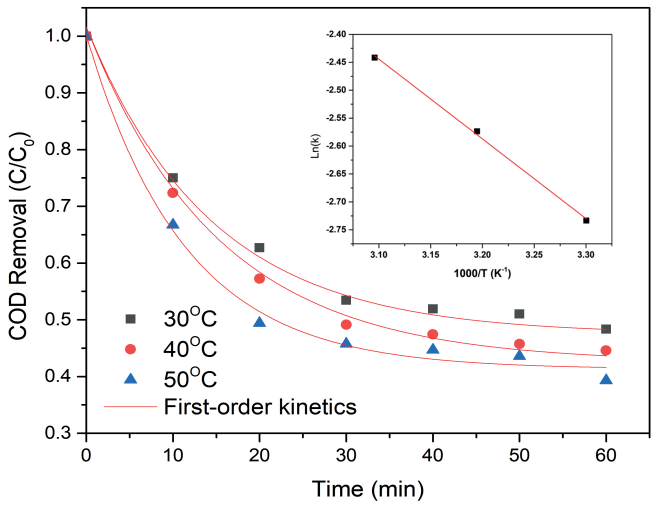

Figure 7. Temperature effect of COD removal of paper mill effluent profiles versus time. Condition of Reaction: C_{CODO} = 1,119 mgL^{-1}; catalyst dosage: 0.3 gL^{-1}; [PMS]: 1.6 gL^{-1}.

4. CONCLUSION

Two catalyst α-MnO_2@Mn_2O_3 and α-MnO_2 were successfully synthesized using two different acid reductor namely tartaric acid and maleic acid. The materials showed different chemical properties as shown in XRD patterns and morphology from SEM imaging, which α-MnO_2@Mn_2O_3 has more well-ordered nano-rod shapes compared to α-MnO_2 which has less defined morphologies. As tartaric acid is stronger reductor than maleic acid, two different oxidation states of manganese (Mn(IV) and Mn(II, III)) could be synthesized. As this study shows two different oxidation states of Mn improved the catalytic efficiency for paper mill effluent COD removal using AOP reactions. The factors affecting COD removal, including PMS concentration, catalyst loading, and reaction temperature, were also examined. The effect of catalyst dosage (0.1 , 0.2 and 0.3 gL^{-1}); PMS dosage(0.4, 0.8, 1.6 gL^{-1}); and temperature (30, 40, and 50°C). The α-MnO_2@Mn_2O_3, which is compromised by Mn(IV) and Mn(II, III), by using 0.3 gL^{-1} α-MnO_2@Mn_2O_3, 1.6 gL^{-1} PMS dosage, at 50°C has the best efficiency with almost 75% COD removal, higher than the α-MnO_2 catalyst. Kinetic studies showed that COD removal is apparent as first order reaction and the activation energy of the α-MnO_2@Mn_2O_3 was obtained to be 11.4 kJ/mol.

ACKNOWLEDGEMENTS

This work was supported by the Ministry of Higher Education, Science, and Technology of the Republic of Indonesia and DIPA Research Projects of Universitas Riau.

CREDIT AUTHOR STATEMENT

Heni Sugesti: Investigation, Data curation Writing-Reviewing and Editing. **Barata Aditya Prawiranegara**: Investigation, Data curation, Formal analysis, Writing-Original draft preparation. **Panca Setia Utama**: Visualization, Data curation, Formal analysis. **Edy Saputra**: Supervision, Conceptualization, Methodology, Writing-Reviewing and Editing.

DECLARATIONS

Conflict of interest The authors declare that they have no known competing financial interests or personal relationships that could have appeared to influence the work reported in this paper.

REFERENCES

[1] Saputra, E., et al., 3D N-doped carbon derived from zeolitic imidazole framework as heterogeneous catalysts for decomposition of pulp and paper mill effluent: Optimization and kinetics study. Environmental Research, 2023. 234: p. 116441.

[2] Kumar, P., et al. Advanced oxidation of pulp and paper industry effluent. in Proceedings of the 2011 International Conference on Environmental and Agriculture Engineering (ICEAE 2011). 2011.

[3] Srinivasan, D., Pulp and paper effluent management. Water Environment Research, 1994. 66(4): p. 417-432.

[4] Hermosilla, D., et al., The application of advanced oxidation technologies to the treatment of effluents from the pulp and paper industry: a review. Environmental Science and Pollution Research, 2015. 22: p. 168-191.

[5] Brink, A., C. Sheridan, and K. Harding, Combined biological and advance oxidation processes for paper and pulp effluent treatment. South African Journal of Chemical Engineering, 2018. 25: p. 116-122.

[6] Esmaeeli, A., et al., A comprehensive review on pulp and paper industries wastewater treatment advances. Industrial & Engineering Chemistry Research, 2023. 62(21): p. 8119-8145.

[7] Gupta, A. and R. Gupta, Treatment and recycling of wastewater from pulp and paper mill. Advances in biological treatment of industrial waste water and their recycling for a sustainable future, 2019: p. 13-49.

[8] Bajpai, P. and P. Bajpai, Biological treatment of pulp and paper mill effluents. Biotechnology for pulp and paper processing, 2018: p. 313-369.

[9] Deng, Y. and R. Zhao, Advanced oxidation processes (AOPs) in wastewater treatment. Current Pollution Reports, 2015. 1: p. 167-176.

[10] Dewil, R., et al., New perspectives for advanced oxidation processes. Journal of environmental management, 2017. 195: p. 93-99.

[11] Garrido-Cardenas, J.A., et al., Wastewater treatment by advanced oxidation process and their worldwide research trends. International Journal of Environmental Research and Public Health, 2020. 17(1): p. 170.

[12] Oturan, M.A. and J.-J. Aaron, Advanced oxidation processes in water/wastewater treatment: principles and applications. A review. Critical reviews in environmental science and technology, 2014. 44(23): p. 2577-2641.

[13] Miklos, D.B., et al., Evaluation of advanced oxidation processes for water and wastewater treatment–A critical review. Water research, 2018. 139: p. 118-131.

[14] Parsons, S., Advanced oxidation processes for water and wastewater treatment. 2004: IWA publishing.

[15] Chen, C., et al., Investigation of heavy oil refinery wastewater treatment by integrated ozone and activated carbon-supported manganese oxides. Fuel Processing Technology, 2014. 124: p. 165-173.

[16] Zaheer, Z. and E.S. Aazam, Anionic-micelles assisted oxidation of tartaric acid by permanganate: A kinetic and mechanistic approach. Journal of Molecular Liquids, 2017. 229: p. 436-442.

[17] Lin, L., et al., Multi-dimensional micro-nano scale manganese oxide catalysts induced chemical-based advanced oxidation processes (AOPs) in environmental applications: a critical review. Chemical Engineering Journal, 2023: p. 145600.

[18] Wang, P., et al., Manganese oxide catalytic materials for degradation of organic pollutants in advanced oxidation processes: A review. Journal of Water Process Engineering, 2024. 66: p. 106048.

[19] Saputra, E., et al., Different crystallographic one-dimensional MnO2 nanomaterials and their superior performance in catalytic phenol degradation. Environmental science & tech-

nology, 2013. 47(11): p. 5882-5887.
[20] Saputra, E., et al., Manganese oxides at different oxidation states for heterogeneous activation of peroxymonosulfate for phenol degradation in aqueous solutions. Applied Catalysis B: Environmental, 2013. 142: p. 729-735.
[21] Saputra, E., et al., Shape-controlled activation of peroxymonosulfate by single crystal α-Mn2O3 for catalytic phenol degradation in aqueous solution. Applied Catalysis B: Environmental, 2014. 154: p. 246-251.
[22] Khan, A., et al., Highly efficient α-Mn 2 O 3@ α-MnO 2-500 nanocomposite for peroxymonosulfate activation: comprehensive investigation of manganese oxides. Journal of Materials Chemistry A, 2018. 6(4): p. 1590-1600.
[23] Huang, J. and H. Zhang, Mn-based catalysts for sulfate radical-based advanced oxidation processes: A review. Environment international, 2019. 133: p. 105141.
[24] Islam, M.A., et al., Manganese oxides and their application to metal ion and contaminant removal from wastewater. Journal of water process engineering, 2018. 26: p. 264-280.
[25] Devi, P., U. Das, and A.K. Dalai, In-situ chemical oxidation: principle and applications of peroxide and persulfate treatments in wastewater systems. Science of the Total Environment, 2016. 571: p. 643-657.
[26] Kan, H., et al., Crystallographic manganese oxides enhanced pyrene contaminated soil remediation in microwave activated persulfate system. Chemical Engineering Journal, 2021. 417: p. 127916.
[27] Utama, P.S., et al., LaMnO3 perovskite activation of peroxymonosulfate for catalytic palm oil mill secondary effluent degradation. Journal of Applied Materials and Technology, 2020. 2(1): p. 27-35.
[28] Dawadi, S., et al., Degradation of Methylene Blue Using Hydrothermally Synthesized α-Manganese Oxide Nanostructures as a Heterogeneous Fenton Catalyst. Journal of Nanomaterials, 2022. 2022(1): p. 3405066.
[29] Lan, D., et al., Synthesis, characterization and microwave transparent properties of Mn 3 O 4 microspheres. Journal of Materials Science: Materials in Electronics, 2019. 30: p. 8771-8776.
[30] Umar, A., et al., Porous Mn2O3 nanorods-based electrode for high-performance electrochemical supercapacitor. Journal of Energy Storage, 2024. 81: p. 110305.
[31] Ilunga, A.K., et al., Isothermic adsorption of morin onto the reducible mesoporous manganese oxide materials surface. Applied Catalysis B: Environmental, 2018. 224: p. 928-939.
[32] Wu, J., et al., Peroxydisulfate-based Non-radical Oxidation of Rhodamine B by Fe-Mn Doped Granular Activated Carbon: Kinetics and Mechanism Study. Chemistry–An Asian Journal, 2024. 19(15): p. e202400482.
[33] Giannakis, S., K.-Y.A. Lin, and F. Ghanbari, A review of the recent advances on the treatment of industrial wastewaters by Sulfate Radical-based Advanced Oxidation Processes (SR-AOPs). Chemical Engineering Journal, 2021. 406: p. 127083.
[34] Du, J., et al., Periodate activation with manganese oxides for sulfanilamide degradation. Water research, 2020. 169: p. 115278.
[35] Nidheesh, P.V., et al., Treatment of textile wastewater by sulfate radical based advanced oxidation processes. Separation and Purification Technology, 2022. 293: p. 1211153.
[36] Saputra, E., et al., Egg-shaped core/shell α-Mn2O3@ α-MnO2 as heterogeneous catalysts for decomposition of phenolics in aqueous solutions. Chemosphere, 2016. 159: p. 351-358.
[37] Zhao, Y.S., et al., Kinetic modeling and efficiency of sulfate radical-based oxidation to remove p-nitroaniline from wastewater by persulfate/Fe3O4 nanoparticles process. Separation and Purification Technology, 2015. 142: p. 182-188.
[38] Zhou, T., et al., Degradation of sulfamethoxazole by MnO2/heat-activated persulfate: kinetics, synergistic effect and reaction mechanism. Chemical Engineering Journal Advances, 2022. 9: p. 100200.
[39] Liu, B., et al., Activation of peroxymonosulfate by cobalt-impregnated biochar for atrazine degradation: The pivotal roles of persistent free radicals and ecotoxicity assessment. Journal of hazardous materials, 2020. 398: p. 122768.
[40] Zhang, D., et al., MOFs-derived magnetic C@ Cu–Ni bimetal particles: An efficient peroxymonosulfate activator for 2, 4, 6-trichlorophenol degradation. Chemosphere, 2021. 269: p. 129394.